

**HIGH FREQUENCY COAXIAL VACUUM FEEDTHROUGHS  
FOR THE STACK CORE STOCHASTIC COOLING SYSTEMS OF THE  
CERN ANTIPROTON ACCUMULATION COMPLEX.**

P. Bramham, C. Metzger.

**Abstract.**

The alumina seal which fills the space between the inner conductor and the outer shield of a coaxial feedthrough is likely to cause reflections at micro-waves frequencies.

As such reflections are strong limitations on the performances of the stack core cooling systems, it is important to minimize their effects by matching the characteristic impedance of the feedthrough over a wide frequency range.

In this note we describe a bakeable (up to 250<sup>o</sup>C), low VWSR feedthrough developed to fit requirements of the 2-4 GHz momentum and the two 4-8 GHz betatronic stochastic cooling systems.

## **INTRODUCTION**

As a part of the ACOL project<sup>1</sup>, the AA stack core stochastic cooling systems were to be changed from their previous 1-2 GHz octave band to the 2-4 GHz octave for the momentum system and to the 4-8 GHz octave for the betatronic ones. For these modifications, new coaxial vacuum feedthroughs were required to pass frequencies up to 8 GHz with little reflection (return loss less than -20 dB; i.e. VSWR < 1.2) in order to discourage unbalance or common mode signals which limit the cooling performances at high frequencies when the harmonic signals overlap the sidebands.

Various means<sup>2, 3</sup> have been proposed to minimize reflections from a dielectric support centring the inner conductor of a coaxial air line. At relatively low frequencies, where all dimensions are small compared with the wavelengths, it is sufficient to compensate for low impedance by adjusting the diameter ratio at the insulator. At higher frequencies, in the GHz range, convenient line sizes are no longer a small part of the wavelength and to have a good impedance match over a wide frequency range, it is then necessary to hold constant the characteristic impedance all along the line, compensating any step discontinuities and their fringing effects as they occur.

## **ISHIMARU FEEDTHROUGH**

Using a parallel resonant support made of two pieces of 50  $\Omega$  line each having two dielectrics (air or vacuum and alumina) arranged concentrically, Ishimaru<sup>4</sup> has obtained a good match up to 6.5 GHz for coaxial vacuum feedthroughs on button-type pickup electrodes in the Tristan storage ring. This structure was also adopted in LEP<sup>5</sup> for a similar application, and preliminary measurements on a test piece showed that such a support could be used at higher frequencies with a few improvements.

## **LIMITATION OF PERFORMANCES**

To hold constant the characteristic impedance along the line, the diameter ratios for the different cross sections of the support are calculated (see Appendix) assuming unperturbed TEM modes; i.e. electric fields everywhere radial. However, at each step in diameter higher modes are excited giving a fringing electric field which stores energy in a si-

milar way that energy is stored in a reactive circuit element and produce transmission losses by reflection. When the fringing field of two or more discontinuities interact, as is the case for the Ishimaru support, more energy is trapped and consequently the losses grow. In practice, those losses could be minimized by staggering the positions of inner and outer steps (Fig. 1) so that the fringing fields set up by each step are in separate regions and, therefore, do not interact with each other.

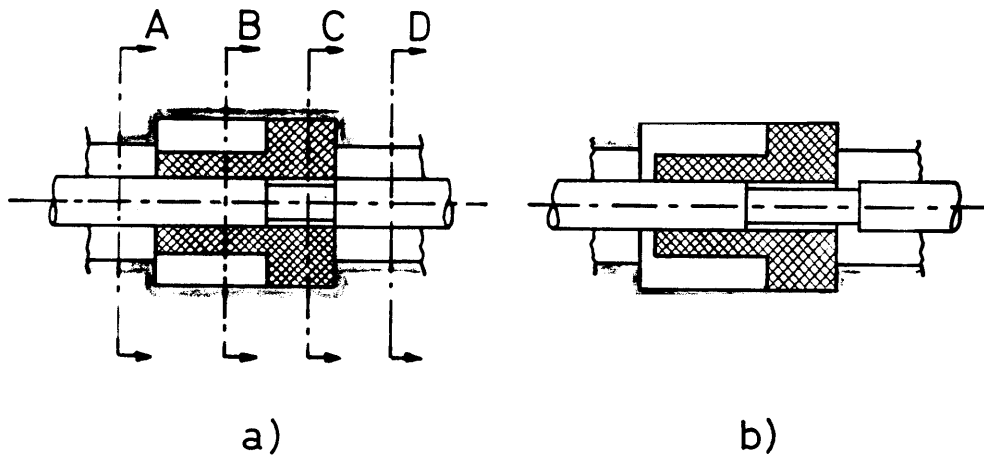
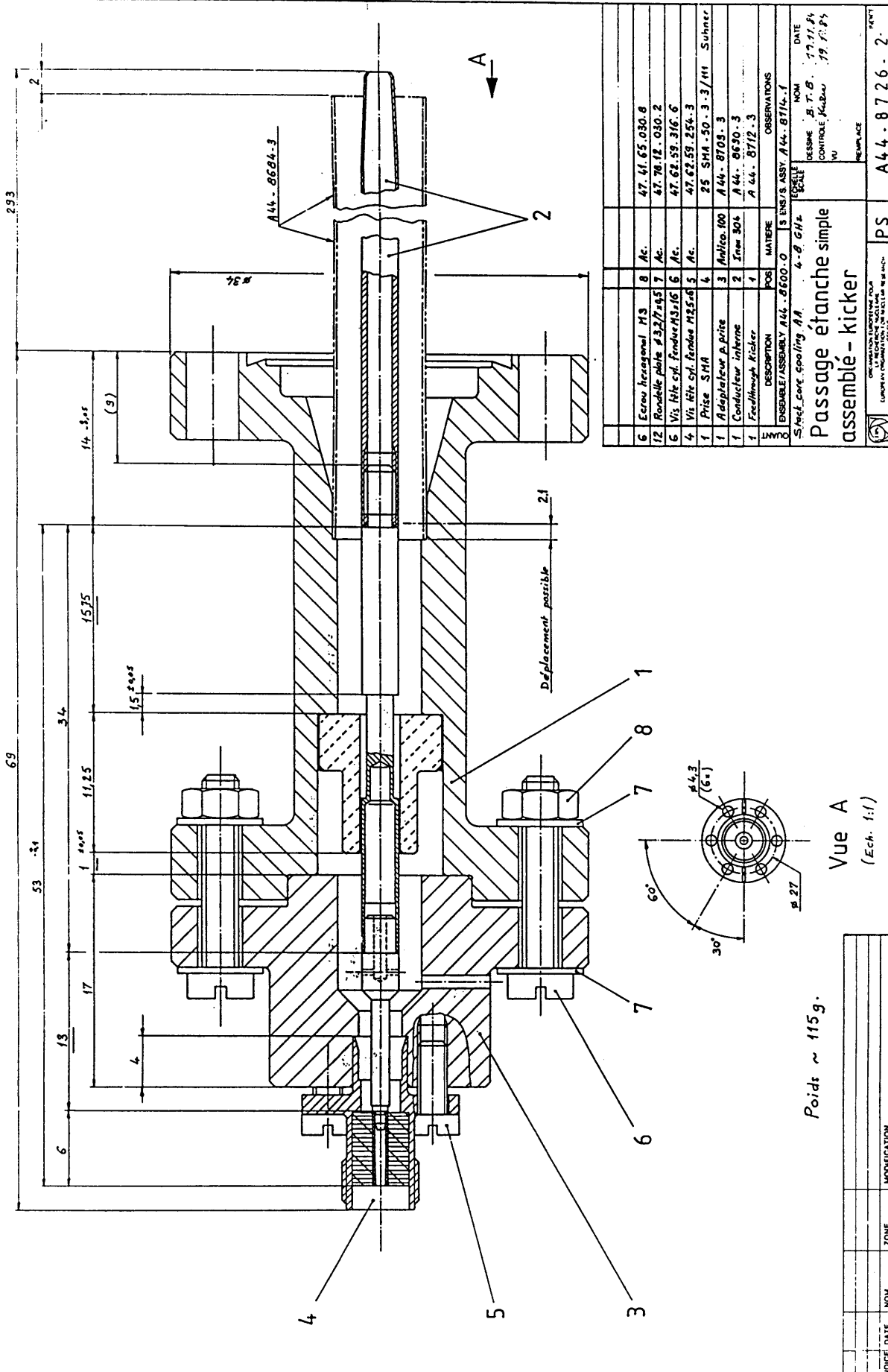


**Fig. 1** - a) Ishimaru support: the diameter ratios for the cross section A, B, C and D are adjusted to give an impedance of 50  $\Omega$ .  
b) The positions of inner and outer steps are staggered to avoid overlapping of their respective fringing fields.

When the wavelengths are comparable to the circumference of the line mean diameter, evanescent waveguide modes may be excited in the annular spacing (air, vacuum or alumina) but will decay more or less rapidly along the line, carrying no real power. Nevertheless, impedance mismatches will appear for the frequency range of these modes and it is essential to keep the support cross section small enough to situate such modes beyond the upper frequency limit of the feedthrough.

### **DESIGN AND CONSTRUCTION**

Figures 2 and 3 show how the feedthrough system is applied to the line coming from the pickups or kickers. At the vacuum end of the body an ultra-high-vacuum, knife-edged standard flange is tapered to facilitate entry of a tube forming the outer conductor of a 50  $\Omega$ , 7 mm/3 mm line. The inner conductor is first screwed in and the line is connected to the



Poids ~ 115g.

Vue A  
(Ech. 1:1)

Q	DESIGNATION	POS	MATIERE	OBSERVATIONS
6	Ecran hexagonal M9	8	Ac.	47.41.65.030.8
12	Rondelle plate #32/45	7	Ac.	47.78.12.030.2
6	Vis file cyl. fendue M3x16	6	Ac.	47.62.59.316.6
4	Vis file cyl. fendue M3.5x8	5	Ac.	47.62.59.256.3
1	Prise SMA	4	25 SMA-50-3-3/411	Suhner
1	Adaptateur A-pite	3	Alnico 100	A44-8708-3
1	Conducteur interne	2	Inox 304	A44-8630-3
1	Feedthrough kicker	1	A 44-8712-3	
1	DISK/ASSEMBLY A44-8500-0	5	EN853 ASBY	A44-8714-1

DESIGNEUR NOM DATE  
 Dessineur B.T.B. 17.11.84  
 CONTRÔLEUR NOM DATE  
 VU 19.10.84  
 REMPLACE

PS A44-8726-2

ORIGINAL DESTROYED FOR  
 SECURITY REASONS  
 LONDON INFORMATION ON SELECTED RESEARCH  
 SECRET

INDICE DATE NOM ZONE MODIFICATION

Fig. 2 - Single feedthrough used on the 2-4 GHz kicker and pickup and on the 4-8 GHz kicker.

PROJETS	REV.	DATE	REVISIONS
1.0	1	1984.11.17	1.0
1.1	1	1984.11.17	1.1
1.2	1	1984.11.17	1.2
1.3	1	1984.11.17	1.3
1.4	1	1984.11.17	1.4
1.5	1	1984.11.17	1.5
1.6	1	1984.11.17	1.6
1.7	1	1984.11.17	1.7
1.8	1	1984.11.17	1.8
1.9	1	1984.11.17	1.9
2.0	1	1984.11.17	2.0
2.1	1	1984.11.17	2.1
2.2	1	1984.11.17	2.2
2.3	1	1984.11.17	2.3
2.4	1	1984.11.17	2.4
2.5	1	1984.11.17	2.5
2.6	1	1984.11.17	2.6
2.7	1	1984.11.17	2.7
2.8	1	1984.11.17	2.8
2.9	1	1984.11.17	2.9
3.0	1	1984.11.17	3.0
3.1	1	1984.11.17	3.1
3.2	1	1984.11.17	3.2
3.3	1	1984.11.17	3.3
3.4	1	1984.11.17	3.4
3.5	1	1984.11.17	3.5
3.6	1	1984.11.17	3.6
3.7	1	1984.11.17	3.7
3.8	1	1984.11.17	3.8
3.9	1	1984.11.17	3.9
4.0	1	1984.11.17	4.0
4.1	1	1984.11.17	4.1
4.2	1	1984.11.17	4.2
4.3	1	1984.11.17	4.3
4.4	1	1984.11.17	4.4
4.5	1	1984.11.17	4.5
4.6	1	1984.11.17	4.6
4.7	1	1984.11.17	4.7
4.8	1	1984.11.17	4.8
4.9	1	1984.11.17	4.9
5.0	1	1984.11.17	5.0
5.1	1	1984.11.17	5.1
5.2	1	1984.11.17	5.2
5.3	1	1984.11.17	5.3
5.4	1	1984.11.17	5.4
5.5	1	1984.11.17	5.5
5.6	1	1984.11.17	5.6
5.7	1	1984.11.17	5.7
5.8	1	1984.11.17	5.8
5.9	1	1984.11.17	5.9
6.0	1	1984.11.17	6.0
6.1	1	1984.11.17	6.1
6.2	1	1984.11.17	6.2
6.3	1	1984.11.17	6.3
6.4	1	1984.11.17	6.4
6.5	1	1984.11.17	6.5
6.6	1	1984.11.17	6.6
6.7	1	1984.11.17	6.7
6.8	1	1984.11.17	6.8
6.9	1	1984.11.17	6.9
7.0	1	1984.11.17	7.0
7.1	1	1984.11.17	7.1
7.2	1	1984.11.17	7.2
7.3	1	1984.11.17	7.3
7.4	1	1984.11.17	7.4
7.5	1	1984.11.17	7.5
7.6	1	1984.11.17	7.6
7.7	1	1984.11.17	7.7
7.8	1	1984.11.17	7.8
7.9	1	1984.11.17	7.9
8.0	1	1984.11.17	8.0
8.1	1	1984.11.17	8.1
8.2	1	1984.11.17	8.2
8.3	1	1984.11.17	8.3
8.4	1	1984.11.17	8.4
8.5	1	1984.11.17	8.5
8.6	1	1984.11.17	8.6
8.7	1	1984.11.17	8.7
8.8	1	1984.11.17	8.8
8.9	1	1984.11.17	8.9
9.0	1	1984.11.17	9.0
9.1	1	1984.11.17	9.1
9.2	1	1984.11.17	9.2
9.3	1	1984.11.17	9.3
9.4	1	1984.11.17	9.4
9.5	1	1984.11.17	9.5
9.6	1	1984.11.17	9.6
9.7	1	1984.11.17	9.7
9.8	1	1984.11.17	9.8
9.9	1	1984.11.17	9.9

DESIGN, FABRICATE TOLERANCES  
 DIMENSIONS IN MILLIMETERS  
 ACCORDING TO ISO STANDARDS

Caution: This drawing may be used for the construction of parts without written authorization.  
 Reproduction interdite sans autorisation écrite.



pickup or kicker module by slotted collets forming an end contact. The outside flange of the body carries an adaptor from the 7 mm/3 mm line to SMA (as shown on the pictures) or type N connectors.

The dimensions of the seal were first checked experimentally using a test piece made of plastic material "Stycast"<sup>6</sup> having about the same dielectric constant as alumina. A few dimensional changes were needed to suit brazing operations.

The body and inner conductor are made of titanium to approximate the expansion coefficient of the alumina. This minimizes deformations during brazing, as well as keeping down risks of cracking the insulator during the 250°C bakeout required for an ultra-high-vacuum environment.

### **BRAZING**

The body and the inner conductor are brazed to the metallized alumina seal in one operation, in a vacuum furnace. To relieve stresses as the unit cools after brazing, the inner conductor is made hollow where it is brazed to the alumina; a vent-hole in the cavity prevents air entrapment.

To preserve correct alignment and relationship between the individual parts, the assembly is vertically supported in a fixture during bonding. The filler alloy in wire ring form is laid along the bevelled edges of the ceramic on the top of the joints.

### **TESTS AND IMPROVEMENTS**

Brazed test pieces were obtained from various sources: some were made at CERN and some by different specialists in France and Germany.

Initially the alumina insulators were moulded and fired to shape but it was found necessary to grind them to get the required tolerances.

Early units showed input reflection coefficient better than -20 dB (VSWR 1.2) over 1-4 GHz range but poor performances from 4-8 GHz. These bad results at high frequencies were due to reactive obstacles formed in the chamfers by a residual fillet of molten alloy (Fig. 4) causing a strong microwave reflection around 6 GHz (-10 dB, VSWR 1.9). Performances were greatly improved by grinding these unwanted fillets. In order to



**Fig. 4 -** Microscopic close-up ( $\times 150$ ) of reactive obstacles formed by residual fillets of brazing alloy, a) inner joint, b) outer joint.

avoid this costly grinding operation, we have successfully tried to bury the brazing alloy wire in a concealed groove within the outer joint, and for the inner one to reduce the volume of the chamfer and to be sparing with the filler material (Fig. 5).

All the feedthroughs used underwent several baking cycles in the laboratory from room temperature to 250°C. No leak was observed during the test and the degassing rate after baking was in the noise signal of our measuring installation.

### **RF MEASUREMENT**

The reflection coefficient was measured from 0.5 to 8.5 GHz by connecting two feedthroughs back-to-back via a 30 cm air line, with a 50  $\Omega$  termination after the second feedthrough. On Fig. 6 we can see narrow notches given by the reflection in the airline between the alumina support of the two feedthroughs and wider ones given by the reflection in the adaptor between the alumina support and the SMA connector.

### **ACKNOWLEDGEMENTS**

This work was encouraged by Colin Taylor and we are grateful to Sten Milner for his expert collaboration in the mechanical design.

### **REFERENCES**

1. E.J.N. Wilson, Editor, Design Study of an Antiproton Collector for the Antiproton Accumulator (ACOL), CERN Report 83-10, 1983.
2. T. Moreno, Microwave Transmission Design Data, Dover, 1958.
3. P. Bramham, Matched Vacuum Window for Coaxial Line, Electronic Engineering, April 1969.
4. H. Ishimaru, Al Alloy-Ceramic Ultrahigh Vacuum and Cryogenic Feed-through Useful from dc to 6.5 GHz, Vacuum, Vol. 32, No. 12, 1982.
5. J. Borer, Technical Specification for 6 Prototype Button Electrodes, CERN Document Y/I-6244/LEP.
6. Stycast: Trade-Mark of Emerson and Cumming, see Technical Bulletin 5.2.2.



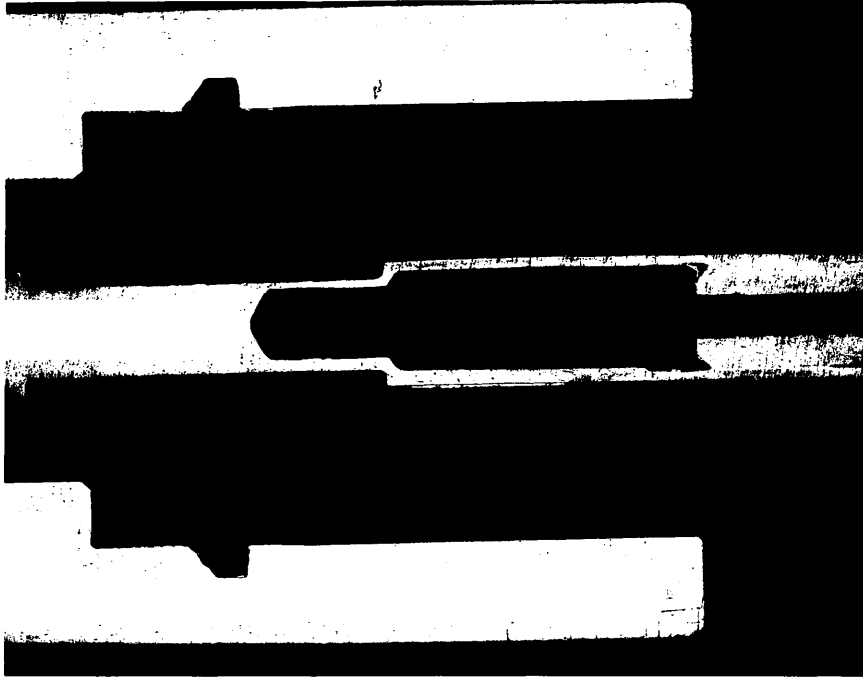


**Fig. 5** - Microscopic close-up ( $\times 5.6$ ) of the modified feedthrough: the brazing alloy is buried in a concealed groove within the outer joint.

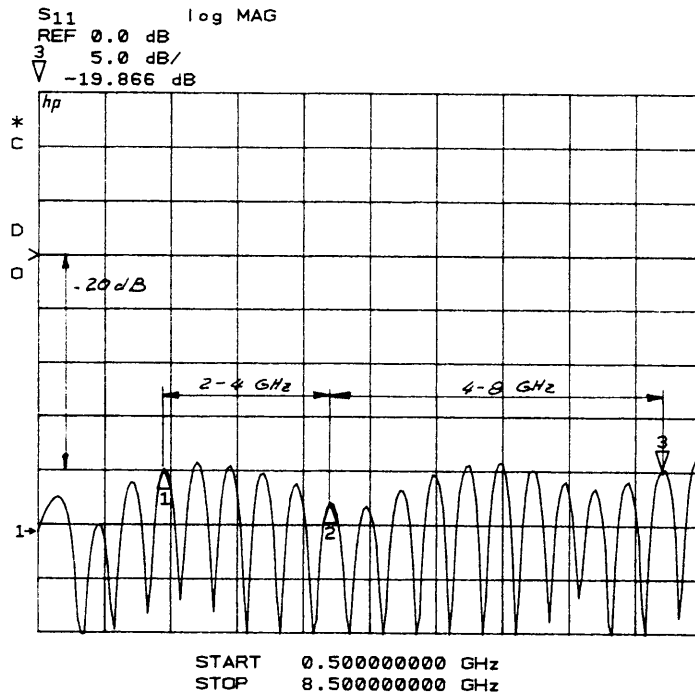
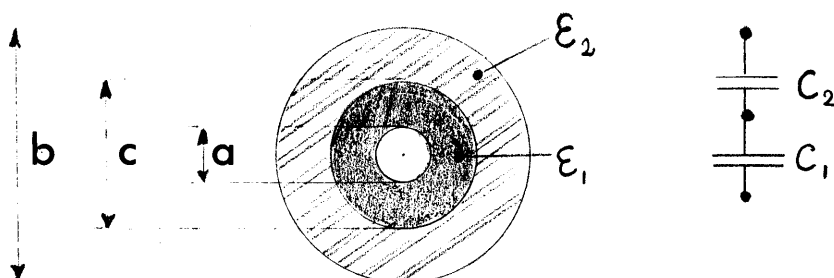


**Fig. 6** - This reflection coefficient curve was measured by connecting two feedthroughs back-to-back via a 30 cm airline, with a 50  $\Omega$  termination after the second feedthrough. The narrow notches are due to the reflection in airline between the alumina support of the feedthroughs. The two wider ones are given by reflection in the adaptor between the alumina support and the SMA connector.

**A P P E N D I X**

**LINE WITH TWO COAXIAL DIELECTRICS**

At planes B and C of the coaxial line shown on Fig. 1 the characteristic impedance of the line is calculated by considering the case of two capacitances in series.



The annular dielectric regions have capacitances respectively

$$C_1 = 2\pi\epsilon_1/\ln(c/a) , \quad C_2 = 2\pi\epsilon_2/\ln(b/c) \quad [F/m]$$

where a and b are the conductor diameters,  
 c is the dielectric boundary diameter,  
 $\epsilon_1, \epsilon_2$  are the respective dielectric constants.

For cross section B,  $\epsilon_1$  corresponds to the insulator, while  $\epsilon_2 = \epsilon_0$  (i.e. free space). For cross section C, these are reversed.

The net capacitance of the line is obtained by adding  $C_1$  and  $C_2$  in series:

$$C_n = \frac{1}{1/C_1 + 1/C_2} = \frac{1}{(1/\epsilon_1)\ln(c/a) + (1/\epsilon_2)\ln(b/c)} \quad [F/m]$$

The inductance of the line is not affected by the dielectric:

$$L = \frac{\mu_0}{2\pi} \ln\left(\frac{b}{a}\right) \quad [H/m]$$

So that the line characteristic impedance is:

$$\begin{aligned}
 Z_0 &= \sqrt{\frac{L}{C_n}} = \frac{\sqrt{\mu_0}}{2\pi} \sqrt{\frac{1}{\epsilon_1} \ln\left(\frac{c}{a}\right) + \frac{1}{\epsilon_2} \ln\left(\frac{b}{c}\right)} \cdot \sqrt{\ln\left(\frac{b}{a}\right)} \\
 &= 60 \sqrt{\frac{\epsilon_0}{\epsilon_1} \ln\left(\frac{c}{a}\right) + \frac{\epsilon_0}{\epsilon_2} \ln\left(\frac{b}{c}\right)} \cdot \sqrt{\ln\left(\frac{b}{a}\right)}
 \end{aligned}$$

Substituting  $\ln(b/c) = \ln(b/a) - \ln(c/a)$ , we can write:

$$\ln\left(\frac{c}{a}\right) = \frac{\epsilon_1 \epsilon_2}{\epsilon_0 (\epsilon_2 - \epsilon_1)} \left[ \frac{(Z_0/60)^2}{\ln(b/a)} - \frac{\epsilon_0}{\epsilon_2} \ln\left(\frac{b}{a}\right) \right]$$

from which c can be calculated to give  $Z_0 = 50\Omega$ . If b and a are known b can be calculated:

$$\ln\left(\frac{c}{a}\right) = \sqrt{\frac{1}{4} \left(1 - \frac{\epsilon_1}{\epsilon_2}\right)^2 \ln^2\left(\frac{b}{c}\right) + \frac{\epsilon_1}{\epsilon_0} \left(\frac{Z_0}{60}\right)^2} - \frac{1}{2} \left(1 + \frac{\epsilon_1}{\epsilon_2}\right) \ln\left(\frac{b}{c}\right)$$